Heliyon 10 (2024) e30555

Contents lists available at ScienceDirect

Heliyon

journal homepage: www.cell.com/heliyon

Research article

Paeoniflorin inhibits the inflammation of rheumatoid arthritis fibroblast-like synoviocytes by downregulating hsa_circ_009012

Junping Yang [a,c], Zehong Wei [c], Huaiyu Li [b,c], Senhao Lv [c], Yong Fu [a,c], Liang Xiao [a,*]

[a] Affiliated Hospital of Jiangxi University of Chinese Medicine, Nanchang, 330006, Jiangxi, People's Republic of China
[b] The First Affiliated Hospital of Guangzhou University of Chinese Medicine, Guangzhou, 510405, Guangdong, People's Republic of China
[c] Jiangxi University of Chinese Medicine, Nanchang, 330006, Jiangxi, People's Republic of China

ARTICLE INFO

Keywords:
Rheumatoid arthritis
Fibroblast-like synoviocytes
Paeoniflorin
TLR4
Has_circ_009012
Inflammation

ABSTRACT

Background: Rheumatoid arthritis (RA) is a chronic inflammatory disease that leads to progressive joint damage. Circular RNA (circRNA) can regulate the inflammatory response of fibroblast-like synoviocytes (FLSs) in RA, influencing the disease progression. Paeoniflorin (PF) is the main active ingredient extracted from Paeonia lactiflora and is known for its anti-inflammatory effect. This study aims to explore the potential mechanisms by which hsa_circ_009012 and PF regulate the inflammatory response in RA.

Methods: RNA expression of hsa_circ_009012, has-microRNA-1286 (miR-1286), toll-like receptor 4 (TLR4), NOD-like receptor thermal protein domain associated protein 3 (NLRP3) was assessed by real-time quantitative polymerase chain reaction (RT-qPCR) or western blotting (WB). Cell inflammation markers (TNF-α, IL-1β, IL-6) were assessed by RT-qPCR and immunofluorescence (IF). Counting Kit-8 (CCK-8) assay, flow cytometry, and transwell assay were utilized to test cell viability, cell cycle distribution, and migration.

Results: Hsa_circ_009012 was highly expressed in RA-FLS. Hsa_circ_009012 over-expression facilitated the inflammation in RA-FLS and was closely associated with the miR-1286/TLR4 axis. Paeoniflorin inhibited inflammation and the expression of hsa_circ_009012 and TLR4, while upregulating the expression of miR-1286 in RA-FLS. Moreover, the upregulation of hsa_circ_009012 reversed the repressive effect of paeoniflorin on RA-FLS progression.

Conclusion: Paeoniflorin inhibits the inflammation of RA-FLS via mediating the hsa_circ_009012/miR-1286/TLR4/NLRP3 axis.

1. Introduction

Rheumatoid arthritis (RA) is a chronic autoimmune disease characterized by symmetric polyarthritis. RA exhibits synovial inflammation which is the fundamental pathological alteration in the early stage of disease, then synovium proliferates and pannus forms that damages joints and impairs joint function, ultimately results in disability in patients with RA [1]. RA is a major global public health challenge, according to the global epidemiological study on RA in 2017, the age-standardized global prevalence and annual incidence rates of RA were 0.246 % and 0.015 %, which show an increasing trend [2,3]. The etiology of RA has not yet been fully clarified, but it generally involves a complex interplay among genetic susceptibility, environmental exposures, microbial infections,

* Corresponding author.
E-mail address: xiaoliang@jxutcm.edu.cn (L. Xiao).

https://doi.org/10.1016/j.heliyon.2024.e30555
Received 27 January 2024; Received in revised form 26 April 2024; Accepted 29 April 2024
Available online 1 May 2024

and immune dysregulation [4,5]. American college of rheumatology guideline for the treatment of rheumatoid arthritis indicates that the treatment of RA includes nonsteroidal anti-inflammatory drugs (NSAIDs), glucocorticoids (GC), conventional synthetic disease-modifying antirheumatic drugs (csDMARDs), biologic DMARDs (bDMARDs) and targeted synthetic DMARDs (tsDMARDs), as well as joint replacement surgery [6,7]. However, in practical clinical treatment, biologic agents and targeted synthetic drugs are more prone to adverse reactions and individual variability in efficacy, coupled with their high cost, which often leads to these treatments not being prioritized as the first-choice options [8–10]. Therefore, finding a safe, effective, and cost-efficient approach to control joint damage caused by RA has become an important goal in treating this disease.

Circular RNAs (circRNAs) are a novel class of non-coding RNAs (ncRNAs) that form a covalently closed loop structure lacking 3′ PolyA tails and 5′ caps, which makes them effectively resistant to degradation by the ribonuclease R (RNase R) [11]. Additionally, circRNAs exhibit characteristics including tissue specificity, conservation, and widespread expression, playing a significant regulatory role in the process of gene expression [12–15]. In recent years, an increasing number of genetic studies related to the pathogenesis of RA (including gene-arrays and new generation sequencing studies) revealed gene expression signatures and networks in synovial tissue and peripheral blood mononuclear cells (PBMCs) [16–18]. Furthermore, research on post-transcriptional mechanisms of gene regulation has identified ncRNAs associated with disease activity, inflammation, pannus formation and bone destruction [19]. These ncRNAs play a significant role in the diagnosis and treatment of RA as biomarkers, mediators of pathogenesis and potential therapeutic targets [19,20].

Paeoniflorin (PF), the main active ingredient in traditional Chinese medicine Paeonia lactiflora, holds significant value in treating RA. PF is widely used to alleviate arthritis symptoms in RA patients, as its anti-inflammatory properties aid in reducing pain and swelling [21]. Furthermore, PF also contributes to slowing down the progression of RA, reducing joint structure damage, and can play a significant role in the long-term management of RA [22]. And PF is considered a relatively safe drug option suitable for patients who experience adverse reactions to conventional treatments or biologics [22]. However, there is currently no literature reporting treatment targeting has_circ_009012 in RA. In previous research, our research team found differential expression of has_circ_009012 in peripheral blood mononuclear cells (PBMCs) between healthy controls and RA patients [16,23], and has_circ_009012 might play a role in the onset and progression of RA by regulating relevant pathways through the targeting of miRNA. This study aims to observe the impact of PF on the expression of has_circ_009012 in RA-FLS, exploring the regulatory mechanism of PF targeting has_circ_009012, thus offering novel insights into PF therapy for RA.

2. Materials and methods

2.1. Cell culture and paeoniflorin treatment

Human fibroblast-like synoviocyte (H-FLS) and RA-FLS cell lines (Jennio Biotechnology, Guangzhou, China) were incubated with Dulbecco's modified Eagle's medium (DMEM; Baikaimei Biotechnology, Shenzhen, China) including 10 % fetal bovine serum (FBS; Procell Life Science&Technology, Wuhan, China) and 1 % penicillin/streptomycin (P/S; Baikaimei Biotechnology, Shenzhen, China). Cells were routinely grown in the humidified condition at 37 °C and 5 % CO_2. For paeoniflorin treatment, RA-FLSs were exposed to various doses (0, 25, 50, 75, 100 and 200 μg/ml) of paeoniflorin (Yuanye Bio-Technology, Shanghai, China) for 24 and 48 h.

2.2. Cell transfection

Small interfering RNA against hsa_circ_009012 (si-circ_009012#1, #2, #3) and scramble control si-NC, hsa_circ_009012 overexpression vector (ad-circ_009012) and its control (pCDH-ciR), miR-1286 mimic and inhibitor and related controls (miR-NC) were synthesized by GeneCreate (Wuhan, China). RA-FLSs were plated into 6-well plates and then transfected with the compositions using Lipofectamine 3000. The transfection efficiency was assessed using RT-qPCR after 48 h post-transfection.

Table 1
Primer sequences used for RT-qPCR.

Gene	Primer sequences	
	Forward (5′–3′)	Reverse (5′–3′)
Has_circ_009012	CTAGAAGCCACCCAAACTGCCAC	GGCCCTCTCCACATAGTCTACCG
TNF-α	GCTTGTTCCTCAGCCTCTTCTCC	GAGGGTTTGCTACAACATGGGCT
IL-1β	CCTGAGCTCGCCAGTGAAATGAT	TTGTCCATGGCCACAACAACTGA
IL-6	CACAGACAGCCACTCACCTCTTC	CAGTGCCTCTTTGCTGCTTTCAC
NLRP3	AGATGGAGTTGCTGTTTGACCCC	ACGCCCAGTCCAACATCATCTTC
TLR4	CCTGGACCTGAGCTTTAATCCCC	AGGGCTAAACTCTGGATGGGGTT
GAPDH	TGACTTCAACAGCGACACCCA	CACCCTGTTGCTGTAGCCAAA
U6	CTCGCTTCGGCAGCACA	AACGCTTCACGAATTTGCGT
Hsa-miR-1286	CGCGTGCAGGACCAAGATG	AGTGCAGGGTCCGAGGTATT
Hsa-miR-1272	GGATGATGATGGCAGCAAATT	AGTGCAGGGTCCGAGGTATT
Hsa-miR-1248	GCGACCTTCTTGTATAAGCACTGT	AGTGCAGGGTCCGAGGTATT

2.3. Reverse-transcription quantitative polymerase chain reaction (RT-qPCR)

Trizol total RNA extraction reagent (TRANS, Beijing, China) for RNA isolation and cDNA first chain synthesis kit (TRANS, Beijing, China) for reverse transcription were carried out as per the instruction books. The quantification detection was conducted through UltraSYBR One Step RT-qPCR Kit (ComWin Biotech, Beijing, China) and miRNA fluorescence quantitative qPCR detection kit (Vazyme Biotech, Nanjing, China). β-actin and U6 were selected as the control genes, and the relative level was analyzed via the $2^{-\Delta\Delta Ct}$ method [24]. The specific primers were provided in Table 1.

2.4. Cell Counting Kit-8 (CCK-8) assay

After transfection for various time points, the viability detection by CCK-8 cell viability assay kit (Baikaimei Biotechnology, Shenzhen, China) was implemented as per the guidelines. RA-FLSs were pipetted with 10 μL CCK-8 reagent and incubated at 37 °C for 1.5 h. The microplate reader was employed for detecting the optical density at 450 nm.

2.5. Cell cycle assay

H-FLSs and RA-FLSs were seeded into 6-well plates at 5×10^5 cells. Each group was set three parallel wells. After 48 h transfection, cells were collected by trypsinization, resuspended thrice in cold PBS and fixed with 75 % ethylalcohol for 6 h at 4 °C. Finally, the distribution of cell cycle was analyzed by flow cytometry (Meilun Biotech, Dalian, China). The percentage of cells in the G1-S and S-G2 phases were analyzed using Modfit software.

2.6. Transwell assay

Cell migration and invasion abilities were assessed via transwell chambers (Corning, NY, USA) pre-coated without or with Matrigel. The treated RA-FLSs were injected into the upper chamber. In the meantime, the lower chamber was filled with 10 % FBS. Then, RA-FLSs were treated with crystal violet. At last, the migrated and invaded cells were calculated under a microscope at 100 × magnification.

2.7. Immunofluorescence (IF) analysis

H-FLSs, non-transfected and transfected RA-FLSs were fixed with 4 % paraformaldehyde for 30 min at room temperature and then permeabilized in PBS containing 0.5 % Triton X-100 on ice for 20 min. The sections were washed with PBS for three times, and immunostained with primary antibodies, and incubated overnight in a wet chamber at 4 °C. The dilutions of antibodies were TNF-α (1:50), IL-1β (1:50), IL-6 (1:50) and NLRP3 (1:50). All antibodies were provided by Biosynthesis biotechnology (Beijing, China). Then, the cells were stained with the corresponding secondary antibody, and incubated at room temperature for 50 min. Cell nuclei were stained with DAPI.

2.8. Western blot (WB)

Protein was extracted using RIPA buffer (Solarbio Science & Technology, Beijing, China) with 1 % protease inhibitor, and concentration was determined with a BCA kit (Biosharp, Anhui, China) following the manufacturer's protocols. The protein sample (10 μg/lane) was separated using sodium dodecyl sulfate-polyacrylamide gel electrophoresis (SDS-PAGE) and transferred onto the polyvinylidene fluoride (PVDF) membrane. Then, the membranes were blocked with 5 % non-fat milk for 1 h, and then incubated with primary antibodies, including TLR4 (ab13556, 1:500 dilution, 96 kDa, Abcam), NLRP3 (ab232401, 1:500 dilution, 118 kDa, Abcam) and GAPDH (ab245355, 1:3000 dilution, Abcam) overnight at 4 °C. Then the membranes were incubated with goat anti-rabbit horseradish peroxidase (HRP)-conjugated secondary antibody (ab205718, 1:8000 dilution, Abcam) for 2 h. Finally, the blots were visualized using ECL reagent (Meilun Biotech, Dalian, China). The grey values of proteins were analyzed utilizing Image J software (NIH, Bethesda, MD, USA). Relative protein expression was normalized to the control group, with GAPDH as a loading control.

2.9. Network pharmacological analysis

The chemical structures and canonical SMILES of PF were obtained from PubChem (https://pubchem.ncbi.nlm.nih.gov/), and the drug targets were identified by the Traditional Chinese Medicine Systems Pharmacology Database and Analysis Platform [25] (TCMSP) (https://tcmsp-e.com/tcmsp.php), the STITCH [26] (http://stitch.embl.de/, ver.5.0) database and the Swiss Target Prediction Database [27] (http://swisstargetprediction.ch/) for drug target prediction analysis, followed by the Genecards [28] database (https://www.genecards.org/) to identify RA disease targets. The UniProt [29] database (https://www.uniprot.org/) was used to normalize gene information and further remove duplicate genes and pseudogenes. Finally, overlapping genes between drug targets and RA targets were extracted for Venn diagramming by R software (version 4.3.1).

The overlapping targets of the predicted targets of PF and RA targets were imported into the STRING [30] database (https://string-db.org), limiting the study species to "*Homo sapiens*". The minimum interaction score was set to 0.400, and the rest parameters were kept at default settings to obtain the PPI network in which PF plays a role in RA. The results were imported into Cytoscape [31]

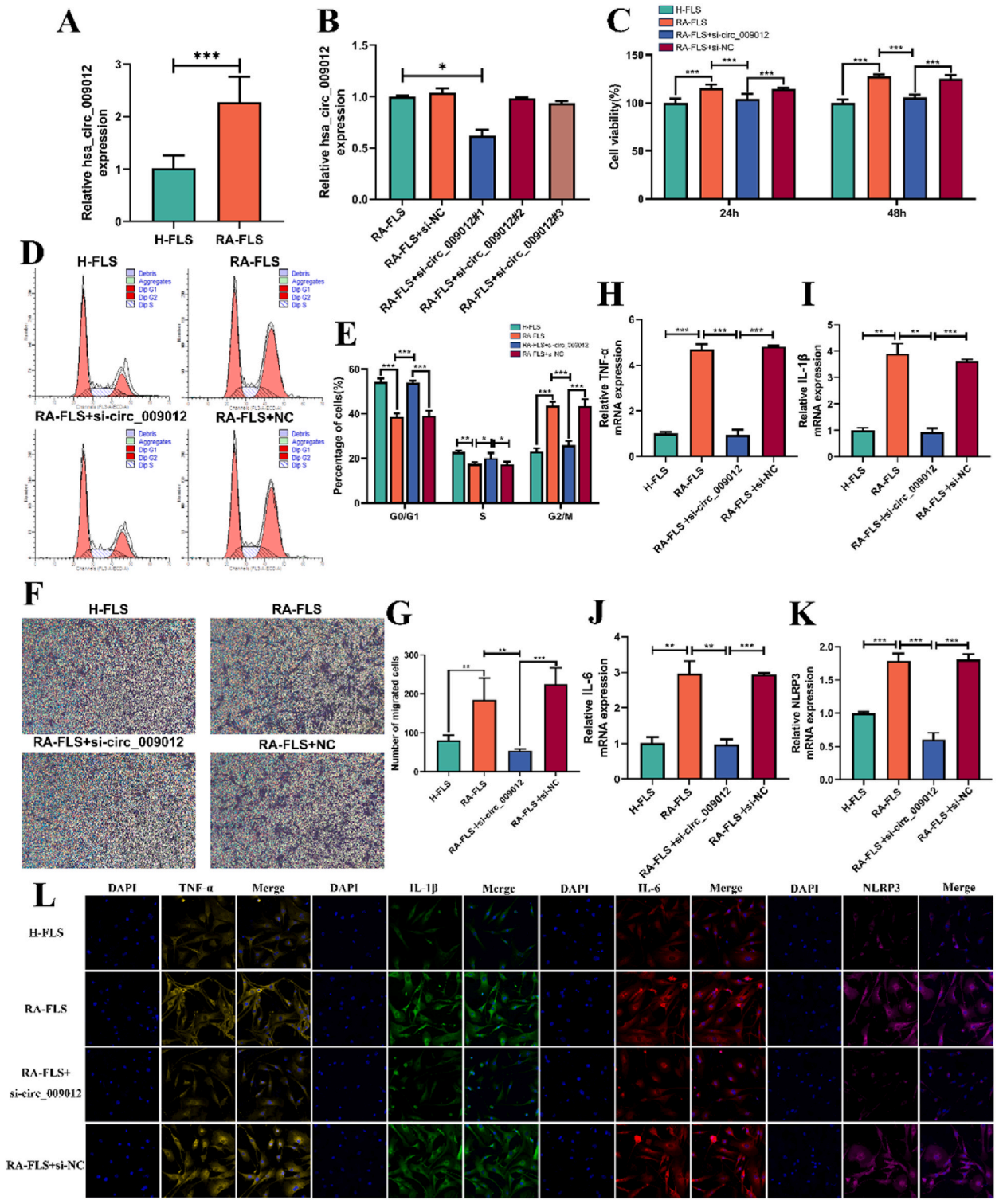

Fig. 1. (A) The expression of hsa_circ_009012 in H-FLSs and RA-FLS was detected by RT-qPCR. (B) RT-qPCR was applied for quantification of hsa_circ_009012 after transfection of si-circ_009012#1, si-circ_009012#2, si-circ_009012#3 and si-NC. (C) CCK-8 assay was used for detecting cell viability detection. (D–E) Flow cytometry was used to analyze cell cycle progression. (F–G) Transwell assay was used to assess cell migration. (H–K) RT-qPCR was used to detect the expression of TNF-α, IL-1β, IL-6, and NLRP3 mRNA. (L) Immunofluorescence was used to detect the expression of TNF-α, IL-1β, IL-6 and NLPRP3.

v.3.10.1, and the node color and size were adjusted according to the degree value to visualize the protein-protein interaction (PPI) network. Additionally, core targets within the PPI network were analyzed by the numbers of interconnected nodes.

The overlapping target genes were converted to their specific Ensembl gene names (www.ensembl.org/biomart/) via the R software. Gene Ontology (GO) and Kyoto Encyclopedia of Genes and Genomes (KEGG) pathway enrichment analysis using the R package "clusterProfile" and "org.Hs.eg.db". Enrichment results were visualized using the "enrichlot" and "ggplot2" R packages. The above-mentioned steps were done by R software 4.3.1 (×64). The final results are presented as bar and bubble plots. P values < 0.05 or q values < 0.05 were considered statistically significant. Molecular functions (MF), biological processes (BP), and cellular components (CC) enriched in overlapping genes were identified by GO analysis, and the top 30 KEGG pathways enriched in overlapping genes were identified by KEGG analysis.

These results were summarized and loaded into Cytoscape v.3.10.1 to construct a PF-target-GO-KEGG-RA network graph. In the network, edges represent interactions between nodes and nodes represent drugs, diseases, pathways, and targets. Additionally, using the Cytoscape plug-in MCODE algorithm to analyze potential protein function modules, with K-Core set to 2.

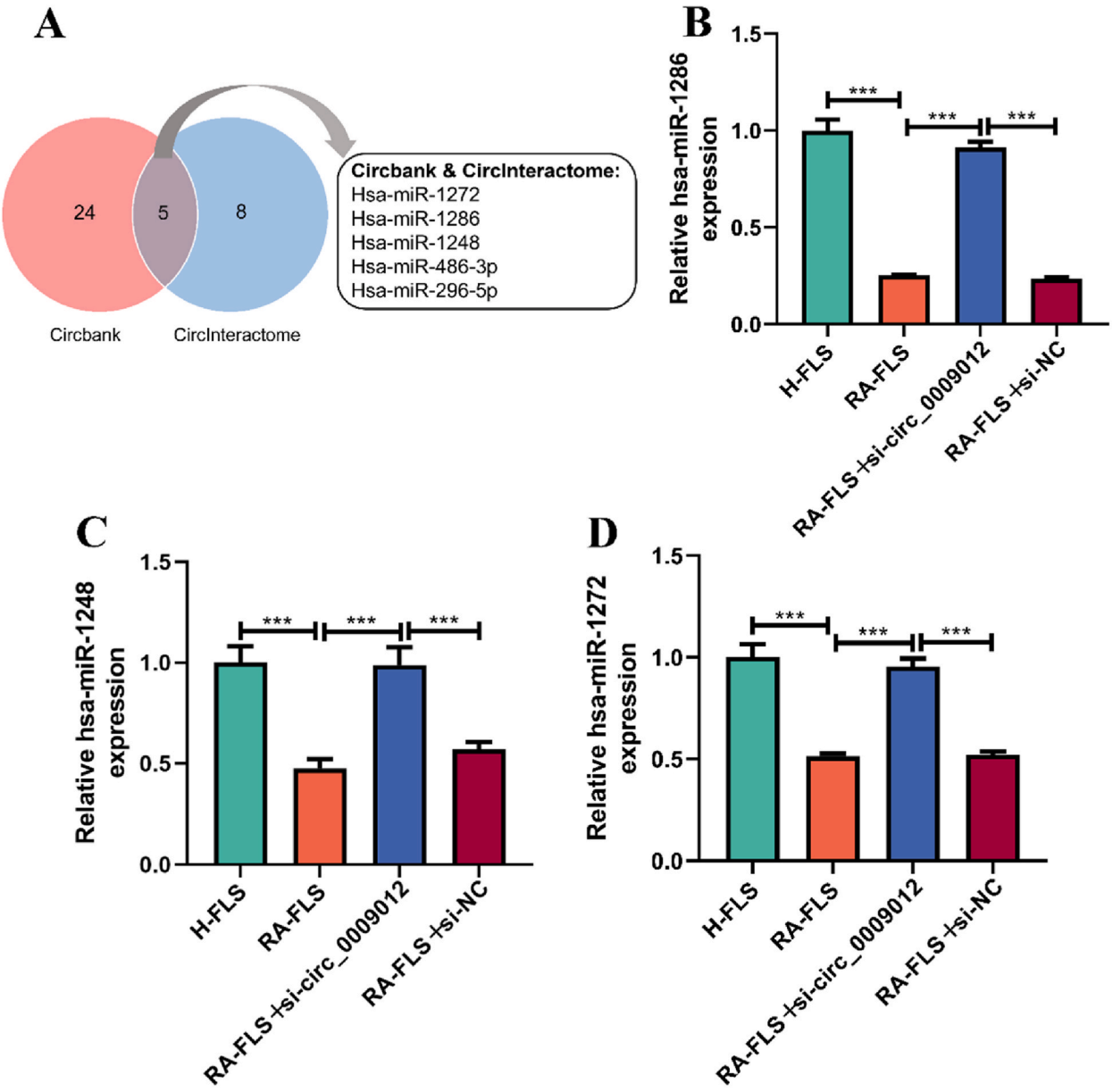

Fig. 2. (A) The miRNA targets from circBank and circinteractome were selected through Venn Diagram. (B–D) RT-qPCR was used to detect the expression of hsa-miR-1272, hsa-miR-1286, and hsa-miR-1248.

2.10. Statistical analysis

The cellular experiments were performed 3 biological replicates with 3 technical replicates. Statistical analysis was conducted using SPSS 27.0 (SPSS Inc., Chicago, IL, USA) and the data were represented as mean ± standard deviation (SD). Difference between

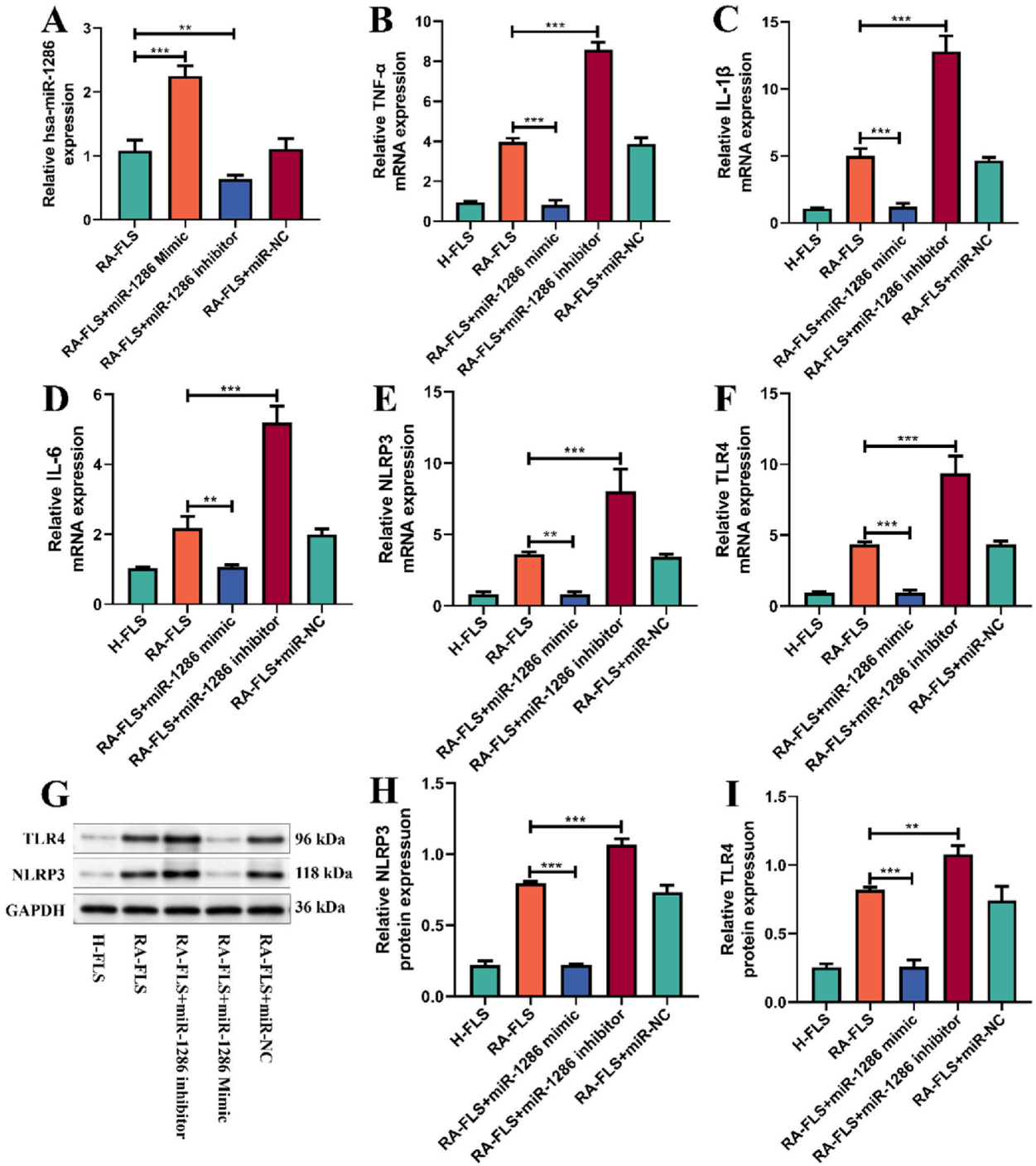

Fig. 3. (A) RT-qPCR was applied for quantification of has-miR-1286 after transfection of miR-1286 mimic and miR-1286 inhibitor and miR-NC. (B–F) RT-qPCR was used to detect the expression of TNF-α, IL-1β, IL-6, NLRP3 and TLR4 mRNA. (G–I) Western blot was used to detect the expression of NLRP3 and TLR4 proteins. For the full, non-adjusted versions of gels and blots of Fig. 3G, please refer to Supplementary Material Fig. S1.

the two groups was analyzed via independent sample *t*-test. Differences between multiple groups were assessed by one-way analysis of variance (ANOVA) followed by Tukey post-hoc test. P value < 0.05 was statistically significant.

3. Result

3.1. Hsa_circ_009012 exhibited a higher level in RA-FLS

The expression of has_circ_009012 was detected by RT-qPCR in cells from H-FLS and RA-FLS groups. Has_circ_009012 showed a significant upregulation in RA-FLS compared to H-FLS, and the difference in Has_circ_009012 expression between the two groups is statistically significant (Fig. 1A). This result is consistent with the expression trend of has_circ_009012 observed in PBMCs from healthy controls and RA patients in our previous studies [16,23].

3.2. Hsa_circ_009012 inhibition repressed cell proliferation, cell cycle progression, cell migration and inflammatory response

RT-qPCR results showed that hsa_circ_009012 was evidently downregulated by si-circ_009012#1 in RA-FLS, contrasted to si-NC group (P $<$ 0.05, Fig. 1B). Therefore, si-circ_009012#1 was chosen for subsequent experiments (hereafter referred to as si-circ_009012). Cell growth analysis by CCK-8 assay demonstrated that cell viability (Fig. 1C) was suppressed after transfection of si-circ_009012. Cell transition from G0/G1 to S phase was prevented by si-circ_009012, suggesting that knockdown of

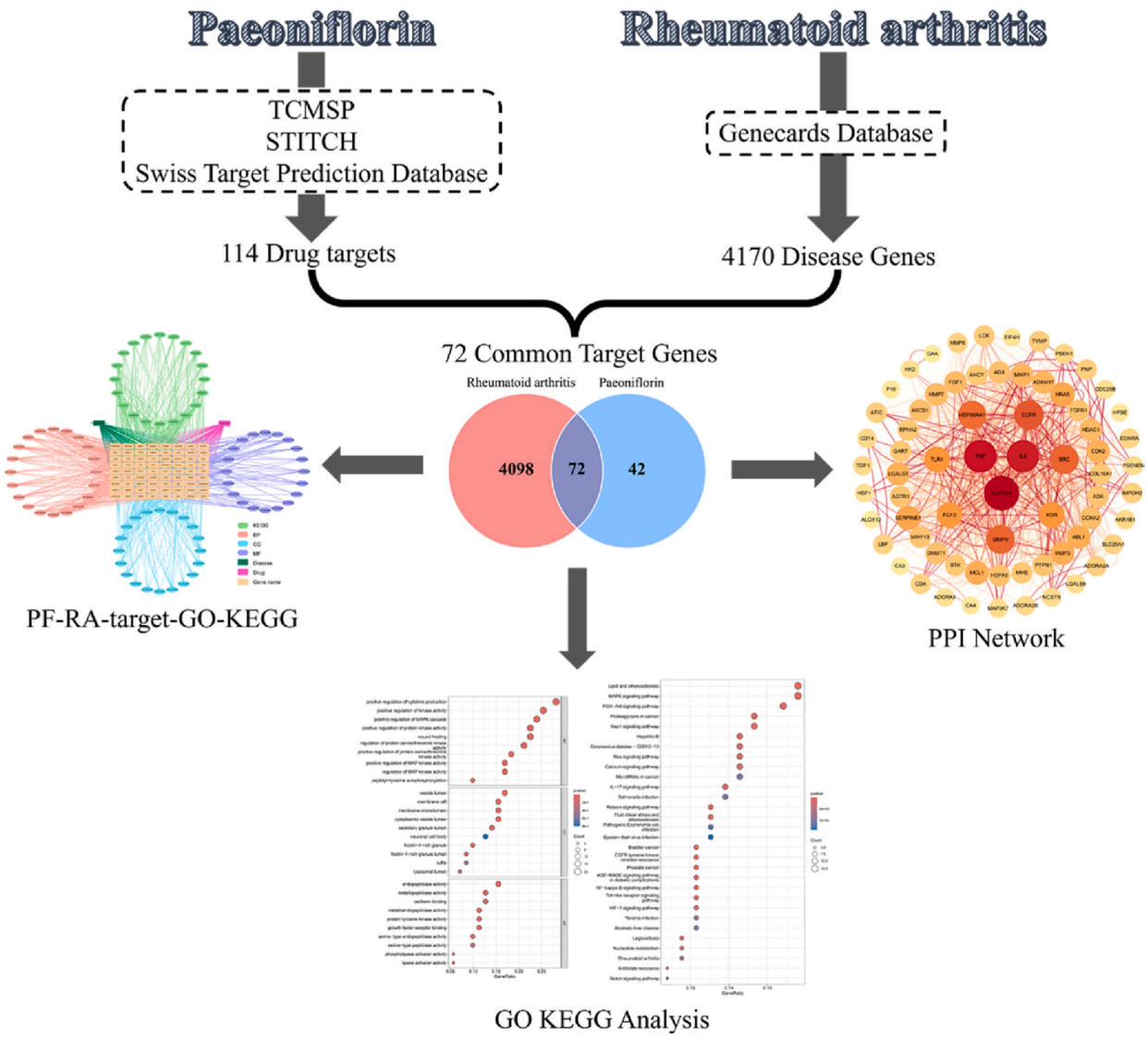

Fig. 4. Framework based on an integration strategy of network pharmacology.

hsa_circ_009012 resulted in cell cycle arrest in RA-FLS (Fig. 1D and E). Cell migration and invasion were investigated by transwell assay. As shown in Fig. 1F and G, hsa_circ_009012 knockdown significantly restrained RA-FLS migration and invasion.

Additionally, RT-qPCR (Fig. 1H–K) and immunofluorescence (Fig. 1L) indicated that hsa_circ_009012 interference significantly reduced the expression of TNF-α, IL-1β, IL-6 and NLPRP3 mRNA in RA-FLS. These data indicated that hsa_circ_009012 knockdown suppressed cell proliferation, cell cycle progression, migration and inflammatory response of RA-FLS.

3.3. *Hsa_circ_009012 interacted with has-miR-1286*

Venn Diagram analysis exhibited that hsa-miR-1272, hsa-miR-1286, hsa-miR-1248, hsa-miR-486-3p and hsa-miR-296-5p were mutually predicted as the targets for circ_0088036 in circBank [32] and circinteractome [33] (Fig. 2A). Then, hsa-miR-1272, hsa--miR-1286, and hsa-miR-1248 were selected for further validation by RT-qPCR in this study. RT-qPCR results (Fig. 2B–D) showed that hsa-miR-1272, hsa-miR-1286, and hsa-miR-1248 were downregulation in RA-FLS, and their expression levels were upregulated after

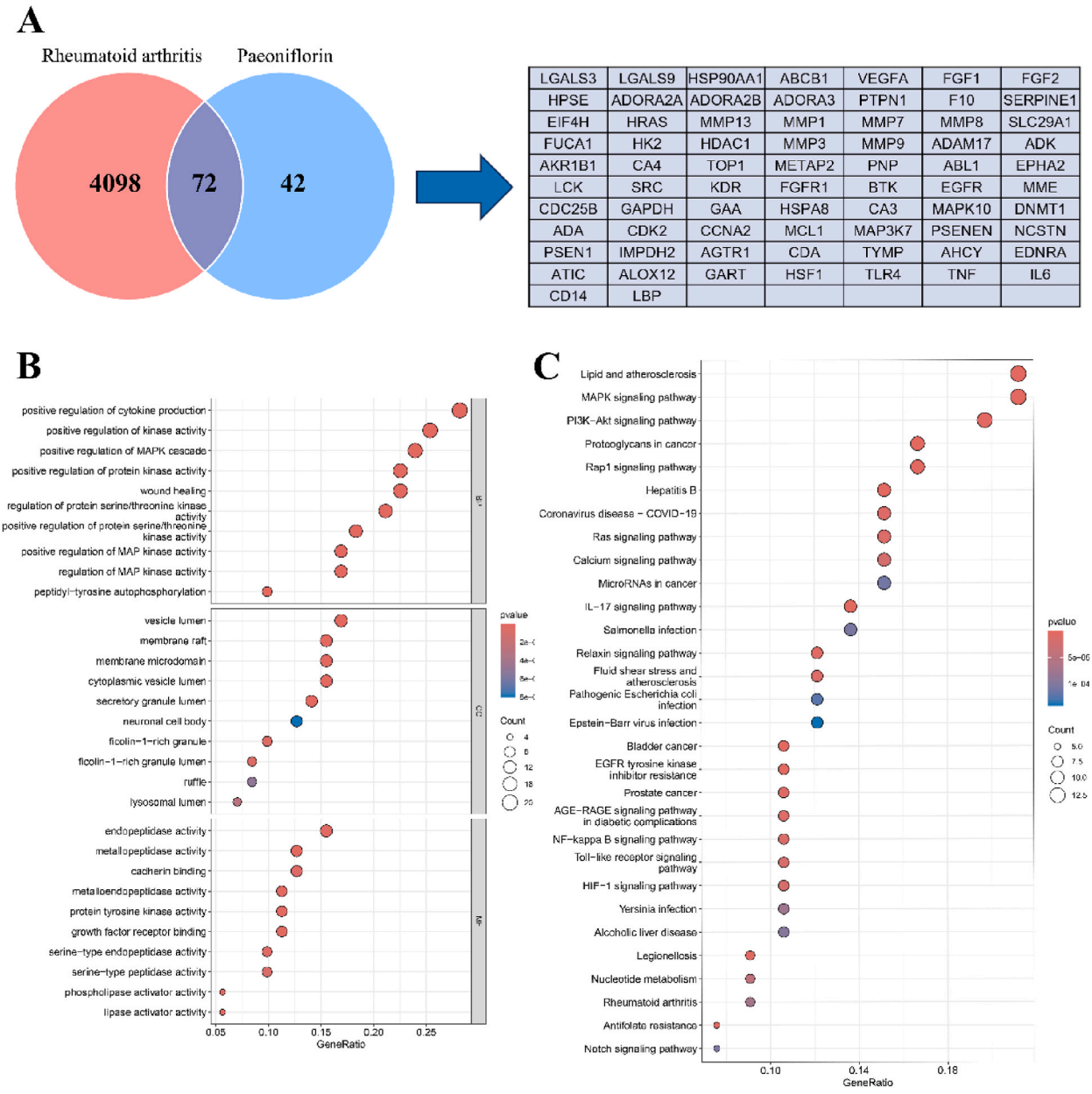

LGALS3	LGALS9	HSP90AA1	ABCB1	VEGFA	FGF1	FGF2
HPSE	ADORA2A	ADORA2B	ADORA3	PTPN1	F10	SERPINE1
EIF4H	HRAS	MMP13	MMP1	MMP7	MMP8	SLC29A1
FUCA1	HK2	HDAC1	MMP3	MMP9	ADAM17	ADK
AKR1B1	CA4	TOP1	METAP2	PNP	ABL1	EPHA2
LCK	SRC	KDR	FGFR1	BTK	EGFR	MME
CDC25B	GAPDH	GAA	HSPA8	CA3	MAPK10	DNMT1
ADA	CDK2	CCNA2	MCL1	MAP3K7	PSENEN	NCSTN
PSEN1	IMPDH2	AGTR1	CDA	TYMP	AHCY	EDNRA
ATIC	ALOX12	GART	HSF1	TLR4	TNF	IL6
CD14	LBP					

Fig. 5. (A) Overlapping genes of PF's potential target and RA disease target (B) GO enrichment results of 72 overlapping genes. (C) KEGG pathway enrichment results of 72 overlapping genes.

knocking down has_circ_009012. This suggests a potential regulatory relationship between has_circ_009012 and hsa-miR-1272, hsa-miR-1286, and hsa-miR-1248. Therefore, hsa-miR-1286, which exhibited the most prominent differential expression, was selected for subsequent studies.

3.4. *Hsa_circ_009012 regulate inflammation in RA-FLS via the miR-1286/TLR4/NLRP3 pathway*

TargetScanHuman8.0 [34] has identified binding sites between hsa-miR-1286 and TLR4. Additionally, TLR4 is closely associated with inflammation and can activate NLRP3 through multiple signaling pathways, thereby promoting the release of inflammatory factors. Therefore, we investigated the mechanism by which hsa-miR-1286 and TLR4 participate in the inflammatory response in RA-FLS by RT-qPCR and Western blot. RT-qPCR has affirmed that miR-1286 mimic transfection for miR-1286 overexpression and miR-1286 inhibitors transfection for miR-1286 inhibition were conspicuous, contrasted to miR-NC control groups (Fig. 3A). Subsequently, RT-qPCR results (Fig. 3B–F) indicated that miR-1286 overexpression and inhibition respectively suppressed and promoted the expression of inflammatory factors (TNF-α, IL-1β, IL-6), TLR4 and NLRP3 mRNA. And the same expression trend of TLR4 and NLRP3 proteins was confirmed by Western blot (Fig. 3G–I).

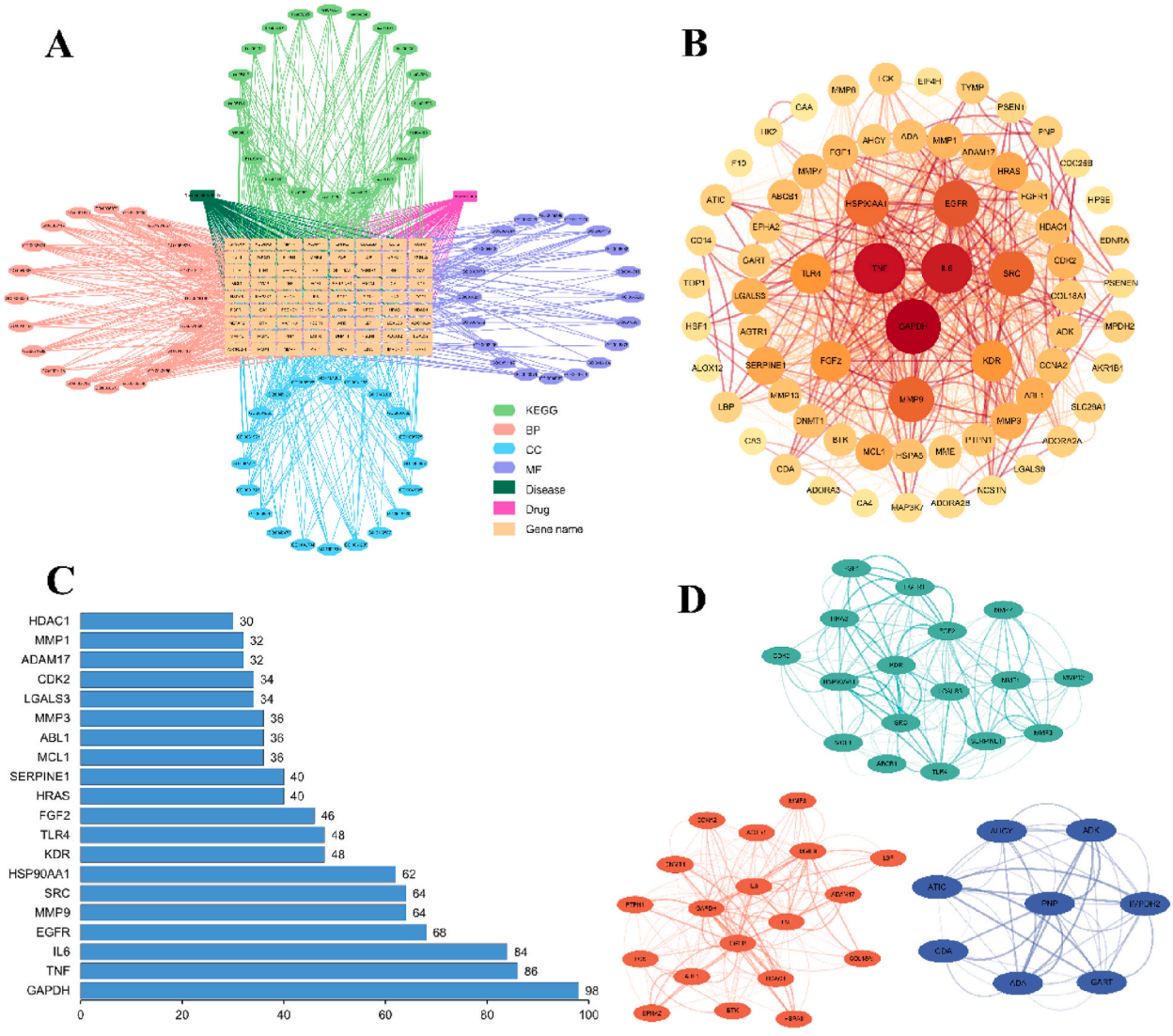

Fig. 6. (A) Network diagram of PF-RA-target-GO-KEGG relationship. (B) PPI network of 72 overlapping genes. (C) Top 20 core genes in the PPI network. (D) The most significant module identified by MCODE plug-in.

3.5. Network pharmacological analysis reveals paeoniflorin regulates TLR4-related signaling pathways in inflammatory responses of RA

Paeonia lactiflora, as a traditional Chinese medicine, has been used for over a thousand years in the treatment of pain, inflammation, and immune system disorders. Total glycoside of paeony (TGP) is extracted from the dried root of Paeonia lactiflora. Paeoniflorin (PF) is the major active component of TGP. Paeoniflorin has been shown to exhibit anti-inflammatory and immunomodulatory effects by restoring abnormal signal transduction in RA-FLS [35]. To further delve into the main signaling pathways involved in the anti-inflammatory effects of PF in RA, detailed study of paeoniflorin was conducted using network pharmacology analysis (Fig. 4).

3.5.1. Potential targets and overlapping genes screening of PF and RA

The targets of PF were searched and predicted by the TCMSP, STITCH, and Swiss Target Prediction Database, resulting in the identification of 114 targets after merging and eliminating duplicate genes. 4170 targets for RA disease were identified by using the Genecards database (set species as "*Homo sapiens*" and gene status as "validated"). After steps such as screening and deduplication, the overlapping genes of PF and RA were limited to 72 (Fig. 5A).

3.5.2. GO and KEGG enrichment analysis and construction of PPI network

GO and KEGG enrichment analysis closely related to PF and RA was performed.

The GO results suggest that biological processes associated with PF treatment of RA included the positive regulation of cytokine production, the positive regulation of MAP kinase activity, the positive regulation of kinase activity, the positive regulation of protein serine/threonine kinase activity, and the positive regulation of protein kinase activity; the associated cellular components included vesicle lumen, membrane raft, membrane microdomain, cytoplasmic vesicle lumen, and secretory granule lumen; the related molecular functions included metalloendopeptidase activity, protein tyrosine kinase activity, growth factor receptor binding, metallopeptidase activity, and endopeptidase activity (Fig. 5B).

The KEGG results showed that the potential mechanisms of PF treatment against RA involved MAPK, PI3K-Akt, Ras, NF-kappa B, Toll-like receptor, IL-17 signaling pathway (Fig. 5C). Based on the abovementioned results, a drug-disease-target-GO-KEGG network map was constructed (Fig. 6A).

Fig. 6B and C shows the PPI network, identifying the top 20 core genes based on the number of interconnected nodes. Additionally, we analyzed the closely connected functional modules in the PPI network using the MCODE function and identified three types of modules with a K-Core value > 2 in the network, as shown in Fig. 6D. These three clusters represent target proteins that are closely related to each other to accomplish specific molecular functions through interactions. Among them, the score for cluster 1 MCODE was 9.357, for nodes was 17, for edges was 150, involving TLR4, FGF2, SRC, and other related target proteins. The score for cluster 2 MCODE was 9.000, for nodes was 19, and for edges was 162, involving GAPDH, TNF, IL6, EGFR, MMP9 and other related target proteins. The score for cluster 3 MCODE was 7.143, for nodes was 8, and for edges was 50, involving ADK, ADA, GATR, and other related target proteins.

In summary, the main signaling pathways involved in the anti-inflammatory effects of PF in RA include the MAPK signaling pathway, PI3K/Akt signaling pathway, NF-κB signaling pathway, and Toll-like receptor signaling pathway. Among these, TLR4 has been identified as the core target through which PF exerts its anti-inflammatory effects in RA. This is related to the signaling pathways through which hsa_circ_009012 regulates the inflammatory response in RA-FLS. Therefore, this study further investigates the relationship between Paeoniflorin's anti-inflammatory effects, Hsa_circ_009012, and its effect on the TLR4 gene.

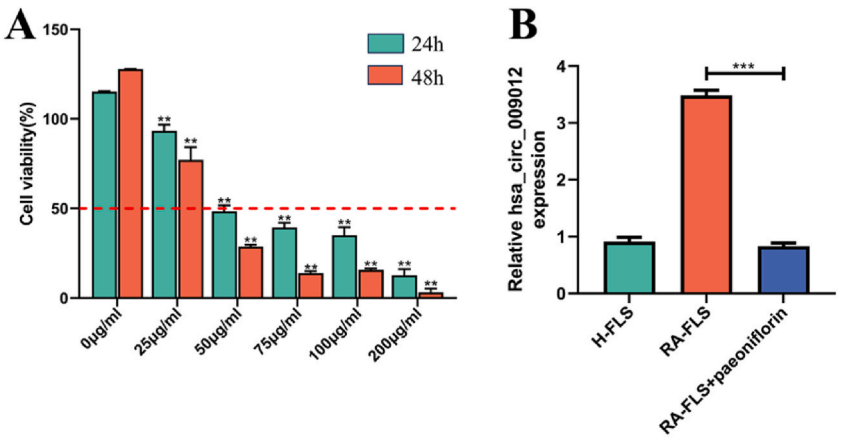

Fig. 7. (A) RA-FLS were stimulated with different doses of paeoniflorin (0, 25, 50, 75, 100,200 μg/ml) for 24 h and 48 h, and cell viability was determined by using CCK-8 analysis. (B) After RA-FLS were treated with paeoniflorin (50 μg/ml) for 24 h, RT-qPCR was used to detect the expression of hsa_circ_009012.

3.6. Paeoniflorin inhibits proliferation and hsa_circ_009012 expression in RA-FLS

To ascertain the role of paeoniflorin in RA progression, RA-FLS were stimulated with different doses of paeoniflorin (0, 25, 50, 75, 100, 200 μg/ml) for 24 h and 48 h. The CCK-8 assay illustrated that paeoniflorin suppressed the viability of RA-FLS dose-dependently

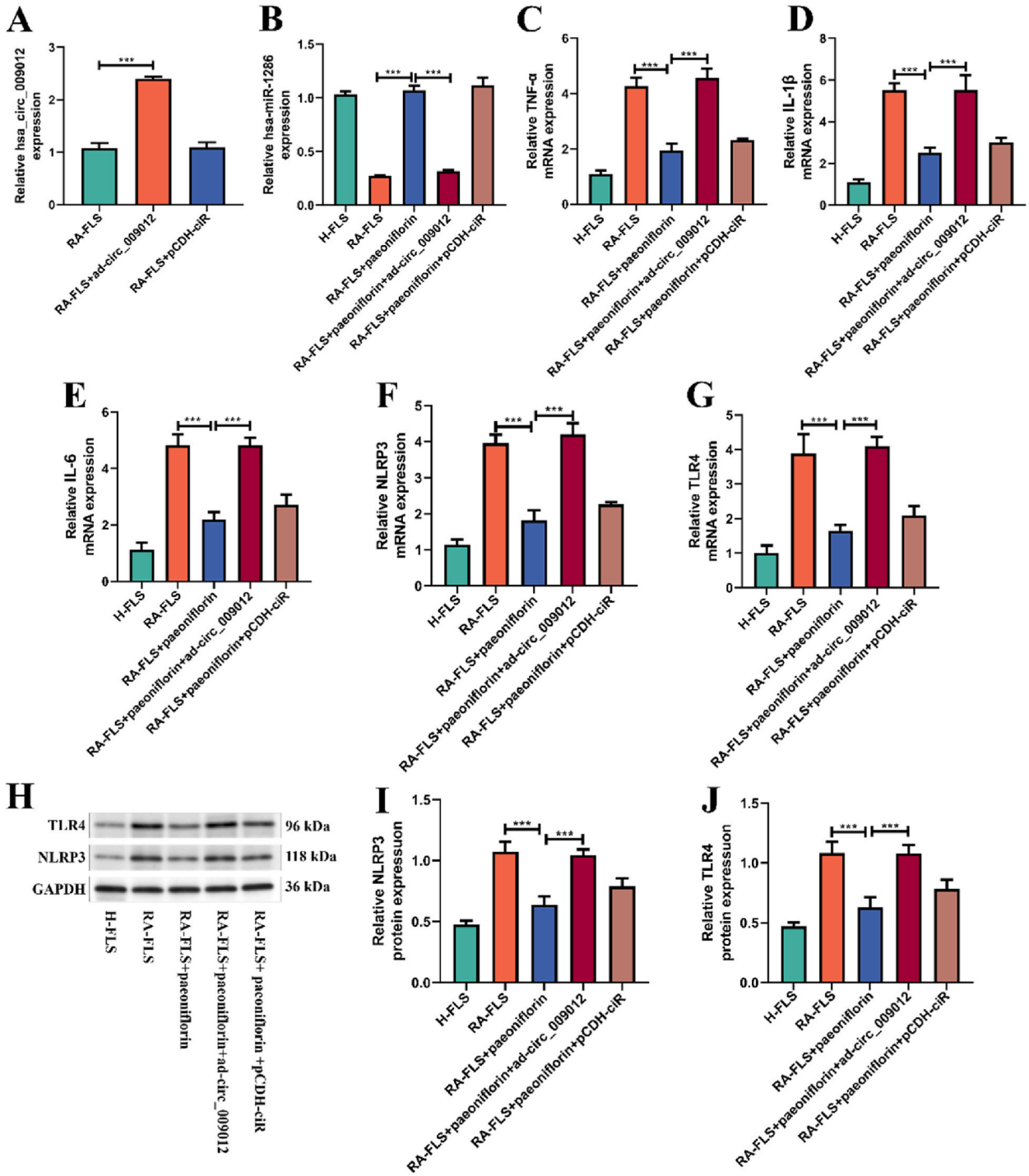

Fig. 8. (A) RT-qPCR was applied for quantification of has_circ_009012 after transfection of ad-circ_009012 and its control (pCDH-ciR). (B–G) After RA-FLS were treated with paeoniflorin (50 μg/ml) for 24 h, RT-qPCR was used to detect the expression of has-miR-1286, TNF-α, IL-1β, IL-6, and NLRP3 mRNA. (H–J) After RA-FLS were treated with paeoniflorin (50 μg/ml) for 24 h, Western blot was used to detect the expression of TLR4 and NLRP3 proteins. For the full, non-adjusted versions of gels and blots of Fig. 8H, please refer to Supplementary Material Fig. S2.

(Fig. 7A). Therefore, 50 μg/ml and 24 h were selected as treatment conditions for paeoniflorin in the following research. Next, RT-qPCR results (Fig. 7B) indicated that paeoniflorin can downregulate the expression of hsa_circ_009012 in RA-FLS.

3.7. Paeoniflorin inhibits inflammation in RA-FLS, while the overexpression of hsa_circ_009012 counters the effects of paeoniflorin in RA-FLS

RT-qPCR has affirmed that ad-circ_009012 transfection for hsa_circ_009012 was conspicuous, contrasted to pCDH-ciR control groups (Fig. 8A). To explore whether hsa_circ_009012 is regulated by paeoniflorin in RA, RA-FLS were introduced with pCDH-ciR or ad-circ_009012 before paeoniflorin administration. RT-qPCR (Fig. 8B–G) and Western blot (Fig. 8H–J) results showed that paeoniflorin suppressed the expression of inflammatory factors (TNF-α, IL-1β, IL-6), TLR4, and NLRP3 mRNA, as well as TLR4 and NLRP3 proteins. Simultaneously, paeoniflorin promoted the expression of has-miR-1286. Additionally, these effects these impacts were abolished by upregulating hsa_circ_009012.

4. Discussion

RA is primarily characterized by autoimmune dysfunction and chronic inflammation [36]. In most cases, the inflammatory process of RA initially affects a single joint, but it commonly progresses to involve nearly all joints [37]. The progression of RA leads to reduced quality of life, bone and cartilage damage, even deformities and disabilities, thereby increasing disability and mortality rates [4]. Therefore, exploring potential therapeutic targets associated with the immunoinflammatory mechanisms in synovial tissue is crucial. The pathophysiology of RA involves various cell types, including FLSs, macrophages, B cells, T cells, chondrocytes, and osteoclasts, all of which participate in the process of joint destruction [38]. Numerous studies suggest that activated FLSs present in the synovium of RA patients are among the key contributors to the joint destruction process [39]. Activated RA-FLS exhibit characteristics similar to tumor cells, including enhanced proliferation, invasion, migration capabilities, and the release of numerous inflammatory factors, which lead to inflammation spread, bone and cartilage destruction, and induction of immune cell infiltration into the synovium [40]. In recent years, extensive studies have revealed that circRNAs play a significant role in regulating gene expression, signaling pathways, or cellular functions of RA-FLS, thereby modulating the onset and progression of RA [41]. This study found that, compared to H-FLSs, has_circ_009012 expression was significantly elevated in RA-FLS, consistent with the expression trend of has_circ_009012 observed in PBMCs from healthy controls and RA patients in our previous studies [16,23]. Additionally, has_circ_009012 may regulate the inflammatory response and biological functions of RA-FLS through a ceRNA mechanism, exacerbating the development of RA.

CircRNAs are ncRNAs that have garnered increasing attention in RA following the exploration of miRNAs and lncRNAs. Compared to traditional linear RNA, circRNAs form a covalently closed loop structure which lacks 3′ PolyA tails and 5′ caps, making them effectively resistant to degradation by the ribonuclease R (RNase R) [11]. Furthermore, circRNAs exhibit characteristics such as tissue specificity, conservation, and ubiquitous expression [12–14,42]. Due to these characteristics, circRNAs hold greater potential as a diagnostic biomarker for diseases [43–46]. Our preliminary studies had explored the circRNA expression profiles in PBMCs of RA patients by microarray assay and receiver operating characteristic (ROC) analysis, then identified hsa_circ_101328 and hsa_circ_009012 exhibit specificity and sensitivity in RA, which indicates that circRNAs hold significant promise as a diagnostic biomarker in RA with broad application prospects [16,23]. Additionally, circRNAs can be modulated by drugs and function by sponging miRNA to reduce the availability of miRNA targeting mRNA. This contributes to mRNA stability or protein expression, thereby impacting the inflammatory response and biological functions of RA-FLS [47–49]. To investigate the role of hsa_circ_009012 in RA-FLS, this study conducted loss-of-function experiments by transfecting RA-FLS with si-circ_009012 and si-NC. The results revealed that knocking down hsa_circ_009012 suppressed the inflammatory response of RA-FLS by reducing the expression of TNF-α, IL-1β, IL-6, and NLRP3 mRNA.

CircRNA can function by sponging miRNA to reduce the abundance of miRNA in the cytoplasm, consequently promoting mRNA translation primarily occurring in the cytoplasm [50]. This study predicted the miRNA targets of hsa_circ_009012 based on the circBank [32] and circinteractome [33], which identifying has-miR-1286 as a potential target of hsa_circ_009012. Subsequently, TargetScanHuman8.0 [34] identified the binding sites between has-miR-1286 and TLR4. To further investigate the role of has-miR-1286 in RA-FLS, we constructed overexpression and inhibition of has-miR-1286 in RA-FLS. RT-qPCR and Western blot results indicated that has-miR-1286 overexpression and inhibition respectively suppressed and promoted the expression of inflammatory factors (TNF-α, IL-1β, IL-6), and NLRP3 by targeting TLR4. Previously, reports have revealed that overexpression of miR-1286 can inhibit the growth of A549 cancer cells in non-small cell lung cancer (NSCLC) [51] and suppress the migration and invasion capabilities of gastric cancer cells [52]. This study similarly found a disease-inhibiting effect when overexpressing miR-1286 in RA-FLS which exhibiting characteristics akin to tumor cells.

Toll-like Receptor 4 (TLR4) is one of the members of the Toll-like receptor family and plays a crucial role in recognizing and responding to pathogens, initiating immune responses [53]. As an upstream regulator of the nuclear factor-kappa B (NF-κB) signaling, TLR4 activates NF-κB, inducing the transcription of NLRP3 and other key pro-inflammatory genes (including proIL-1β) [54,55]. TLR4 can also activate NLRP3 through the receptor-interacting protein 1 (RIP1)-FAS-associated death domain protein (FADD)-caspase 8 pathway, promoting the release of pro-inflammatory mediators (such as IL-1β, IL-18), leukotrienes, and prostaglandins [56]. Our study found that overexpressing has-miR-1286 might suppress the inflammatory response of RA-FLS by reducing the expression of TNF-α, IL-1β, IL-6, and NLRP3 through TLR4. Therefore, hsa_circ_009012 might regulate the inflammatory response of RA-FLS by targeting the has-miR-1286/TLR4/NLRP3 axis.

Furthermore, abundant studies had indicated that paeoniflorin, owing to its anti-inflammatory effects, plays a significant role in

various inflammatory diseases, including RA, and had been verified to ameliorate aberrant biological functions in RA-FLS [21,35,57,58]. This study observed high expression of hsa_circ_009012 in RA-FLS, which was downregulated after paeoniflorin intervention. As there is currently no literature documenting the relationship between paeoniflorin and hsa_circ_009012, our study focused on the anti-inflammatory effects of paeoniflorin. RT-qPCR and Western blot results revealed that paeoniflorin exhibits an anti-inflammatory effect by downregulating the expression of hsa_circ_009012, has-miR-1286, TNF-α, IL-1β, IL-6, TLR4, and NLRP3 in RA-FLS. Additionally, the overexpression of hsa_circ_009012 reversed the anti-inflammatory effect of paeoniflorin in RA-FLS. This aligns with previous research, which reported that intervention with paeoniflorin suppressed the inflammatory response, proliferation, migration, and invasion capabilities of RA-FLS [35]. These findings suggest that paeoniflorin may inhibit the inflammatory response of RA-FLS through the hsa_circ_009012/has-miR-1286/TLR4/NLRP3 axis.

5. Conclusion

This study conducted in vitro cultivation of RA-FLS and observed the overexpression of hsa_circ_009012, which facilitated inflammatory responses in RA-FLS. Furthermore, it is likely that hsa_circ_009012 may regulate the inflammatory response of RA-FLS through the has-miR-1286/TLR4/NLRP3 axis. This suggests that hsa_circ_009012 may modulate the gene and protein expression of RA-FLS via ceRNA mechanism, which could lead to two main effects: on one hand, impacting the release of inflammatory factors by RA-FLS, thereby recruiting additional immune cells from the immune system, resulting in the initiation of an inflammatory loop; on the other hand, influencing the proliferation, invasion, and migration abilities of RA-FLS, intensifying the spread of inflammation. Therefore, hsa_circ_009012 plays a crucial regulatory role in the pathophysiological process of RA, closely associated with the onset and progression of this disease. Additionally, paeoniflorin was found to downregulate hsa_circ_009012 and suppress the inflammatory response of RA-FLS via the has-miR-1286/TLR4/NLRP3 axis, thereby controlling the progression of RA.

6. Limitations

This study is an initial exploration of hsa_circ_009012 in RA-FLS. However, due to experimental constraints, several limitations need to be addressed: (1) the use of cell lines instead of fresh tissues and (2) the absence of other disease controls. Consequently, the intricate cell-cell interactions present in original tissues might be lost, potentially leading to alterations in cell phenotypes and gene expression profiles. Additionally, the lack of comparison with synovial tissues from other relevant diseases weakens the evidence for the specific role of hsa_circ_009012 in RA-FLS. To address these limitations, we aim to undertake a comprehensive and in-depth investigation into the involvement of hsa_circ_009012 in the pathogenesis and treatment of RA. Therefore, future research will involve the evaluation of fresh synovial tissues obtained from untreated or treated RA patients, particularly with paeoniflorin, as well as from individuals with other rheumatic diseases such as SLE. Through these investigations, we aim to enhance the strength and specificity of our findings and further explore the regulatory network involving circRNA/miRNA/mRNA.

Data availability statement

Regarding data availability, Q1 (question1): Has data associated with your study been deposited into a publicly available repository? A1(Authors response): No; Q2: Has data associated with your study been deposited into a publicly available repository? A2: Data will be made available on request; In brief, the original contributions presented in the study are included in the article/supplementary material. Further inquiries can be directed to the corresponding author.

Funding

This work was supported by the National Natural Science Foundation of China (81460769), Jiangxi Provincial Department of Education Scientific and Technological Research Project (GJJ2200935), the Development Plan of Jiangxi University of Traditional Chinese Medicine's School-Level Scientific and Technological Innovation Team (CXTD22012), 2023 Jiangxi University of Traditional Chinese Medicine Graduate Innovation Special Fund Project (JZYC23S12).

Publisher's note

All claims expressed in this article are solely those of the authors and do not necessarily represent those of their affiliated organizations, or those of the publisher, the editors and the reviewers. Any product that may be evaluated in this article, or claim that may be made by its manufacturer, is not guaranteed or endorsed by the publisher.

CRediT authorship contribution statement

Junping Yang: Writing – review & editing, Writing – original draft, Funding acquisition. **Zehong Wei:** Writing – original draft, Funding acquisition, Data curation. **Huaiyu Li:** Writing – review & editing, Project administration, Investigation. **Senhao Lv:** Writing – original draft, Validation, Project administration, Data curation. **Yong Fu:** Writing – review & editing, Funding acquisition. **Liang Xiao:** Writing – review & editing, Funding acquisition.

Declaration of competing interest

The authors declare that they have no known competing financial interests or personal relationships that could have appeared to influence the work reported in this paper.

Appendix A. Supplementary data

Supplementary data to this article can be found online at https://doi.org/10.1016/j.heliyon.2024.e30555.

References

[1] J.S. Smolen, D. Aletaha, A. Barton, et al., Rheumatoid arthritis, Nat. Rev. Dis. Prim. 4 (2018) 18001.
[2] S. Safiri, A.A. Kolahi, D. Hoy, et al., Global, regional and national burden of rheumatoid arthritis 1990-2017: a systematic analysis of the Global Burden of Disease study 2017, Ann. Rheum. Dis. 78 (11) (2019) 1463–1471.
[3] T. Otón, L. Carmona, The epidemiology of established rheumatoid arthritis, Best Pract. Res. Clin. Rheumatol. 33 (5) (2019) 101477.
[4] J.S. Smolen, D. Aletaha, I.B. Mcinnes, Rheumatoid arthritis, Lancet 388 (10055) (2016) 2023–2038.
[5] I.B. Mcinnes, G. Schett, The pathogenesis of rheumatoid arthritis, N. Engl. J. Med. 365 (23) (2011) 2205–2219.
[6] L. Fraenkel, J.M. Bathon, B.R. England, et al., American college of rheumatology guideline for the treatment of rheumatoid arthritis, Arthritis Rheumatol. 73 (7) (2021) 1108–1123, 2021.
[7] S.M. Goodman, B. Springer, G. Guyatt, et al., American college of rheumatology/American association of hip and knee surgeons guideline for the perioperative management of antirheumatic medication in patients with rheumatic diseases undergoing elective total hip or total knee arthroplasty, Arthritis Rheumatol. 69 (8) (2017) 1538–1551, 2017.
[8] P.H. Hsieh, O. Wu, C. Geue, et al., Economic burden of rheumatoid arthritis: a systematic review of literature in biologic era, Ann. Rheum. Dis. 79 (6) (2020) 771–777.
[9] M.C. Genovese, K. Kalunian, J.E. Gottenberg, et al., Effect of filgotinib vs placebo on clinical response in patients with moderate to severe rheumatoid arthritis refractory to disease-modifying antirheumatic drug therapy: the FINCH 2 randomized clinical trial, JAMA 322 (4) (2019) 315–325.
[10] J.D. Cañete, M.V. Hernández, R. Sanmartí, Safety profile of biological therapies for treating rheumatoid arthritis, Expet Opin. Biol. Ther. 17 (9) (2017) 1089–1103.
[11] L.L. Chen, L. Yang, Regulation of circRNA biogenesis, RNA Biol. 12 (4) (2015) 381–388.
[12] I.L. Patop, S. Wüst, S. Kadener, Past, present, and future of circRNA, Embo j 38 (16) (2019) e100836.
[13] L.S. Kristensen, M.S. Andersen, L.V.W. Stagsted, et al., The biogenesis, biology and characterization of circular RNAs, Nat. Rev. Genet. 20 (11) (2019) 675–691.
[14] X. Li, L. Yang, L.L. Chen, The biogenesis, functions, and challenges of circular RNAs, Mol. Cell 71 (3) (2018) 428–442.
[15] S.P. Barrett, J. Salzman, Circular RNAs: analysis, expression and potential functions, Development 143 (11) (2016) 1838–1847.
[16] H. Lu, Y. Yang, D. Kuang, et al., Expression profile of circRNA in peripheral blood mononuclear cells of patients with rheumatoid arthritis, BMC Med. Genom. 15 (1) (2022) 77.
[17] D. Xu, Y. Jiang, L. Yang, et al., Long noncoding RNAs expression profile and functional networks in rheumatoid arthritis, Oncotarget 8 (56) (2017) 95280–95292.
[18] M. Taheri, R. Eghtedarian, M.E. Dinger, et al., Dysregulation of non-coding RNAs in Rheumatoid arthritis, Biomed. Pharmacother. 130 (2020) 110617.
[19] S.A. Ali, M.J. Peffers, M.J. Ormseth, et al., The non-coding RNA interactome in joint health and disease, Nat. Rev. Rheumatol. 17 (11) (2021) 692–705.
[20] C. Li, Y.Q. Ni, H. Xu, et al., Roles and mechanisms of exosomal non-coding RNAs in human health and diseases, Signal Transduct. Targeted Ther. 6 (1) (2021) 383.
[21] L. Zhang, W. Wei, Anti-inflammatory and immunoregulatory effects of paeoniflorin and total glucosides of paeony, Pharmacol. Ther. 207 (2020) 107452.
[22] X. Wang, D. Liu, G. Cui, et al., Circ_0088036 mediated progression and inflammation in fibroblast-like synoviocytes of rheumatoid arthritis by miR-1263/REL-activated NF-κB pathway, Transpl. Immunol. 73 (2022) 101604.
[23] Q. Nie, H. Lu, X. Li, et al., Expression profile of circRNA in peripheral blood mononuclear cells of patients with rheumatoid arthritis, Chinese Journal of Rheumatology (1) (2022) 32, 36, C2. (in Chinese).
[24] K.J. Livak, T.D. Schmittgen, Analysis of relative gene expression data using real-time quantitative PCR and the 2(-Delta Delta C(T)) Method, Methods 25 (4) (2001) 402–408.
[25] J. Ru, P. Li, J. Wang, et al., TCMSP: a database of systems pharmacology for drug discovery from herbal medicines, J. Cheminf. 6 (2014) 13.
[26] D. Szklarczyk, A. Santos, C. Von Mering, et al., Stitch 5: augmenting protein-chemical interaction networks with tissue and affinity data, Nucleic Acids Res. 44 (D1) (2016) D380–D384.
[27] A. Daina, O. Michielin, V. Zoete, SwissTargetPrediction: updated data and new features for efficient prediction of protein targets of small molecules, Nucleic Acids Res. 47 (W1) (2019) W357–w364.
[28] G. Stelzer, N. Rosen, I. Plaschkes, et al., The GeneCards suite: from gene data mining to disease genome sequence analyses, Curr Protoc Bioinformatics 54 (2016), 1.30.1-1.30.33.
[29] UniProt: the universal protein knowledgebase in 2023, Nucleic Acids Res. 51 (D1) (2023) D523–d531.
[30] D. Szklarczyk, R. Kirsch, M. Koutrouli, et al., The STRING database in 2023: protein-protein association networks and functional enrichment analyses for any sequenced genome of interest, Nucleic Acids Res. 51 (D1) (2023) D638–d646.
[31] P. Shannon, A. Markiel, O. Ozier, et al., Cytoscape: a software environment for integrated models of biomolecular interaction networks, Genome Res. 13 (11) (2003) 2498–2504.
[32] M. Liu, Q. Wang, J. Shen, et al., Circbank: a comprehensive database for circRNA with standard nomenclature, RNA Biol. 16 (7) (2019) 899–905.
[33] D.B. Dudekula, A.C. Panda, I. Grammatikakis, et al., CircInteractome: a web tool for exploring circular RNAs and their interacting proteins and microRNAs, RNA Biol. 13 (1) (2016) 34–42.
[34] S.E. Mcgeary, K.S. Lin, C.Y. Shi, et al., The biochemical basis of microRNA targeting efficacy, Science 366 (6472) (2019).
[35] J. Ma, Q. Meng, J. Zhan, et al., Paeoniflorin suppresses rheumatoid arthritis development via modulating the circ-fam120a/miR-671-5p/MDM4 Axis, Inflammation 44 (6) (2021) 2309–2322.
[36] C.M. Weyand, New insights into the pathogenesis of rheumatoid arthritis, Rheumatology 39 (Suppl 1) (2000) 3–8.
[37] S. Lefèvre, A. Knedla, C. Tennie, et al., Synovial fibroblasts spread rheumatoid arthritis to unaffected joints, Nat. Med. 15 (12) (2009) 1414–1420.
[38] M.I. Edilova, A. Akram, A.A. Abdul-Sater, Innate immunity drives pathogenesis of rheumatoid arthritis, Biomed. J. 44 (2) (2021) 172–182.
[39] T. Pap, U. Müller-Ladner, R.E. Gay, et al., Fibroblast biology. Role of synovial fibroblasts in the pathogenesis of rheumatoid arthritis, Arthritis Res. 2 (5) (2000) 361–367.
[40] C. Ospelt, Synovial fibroblasts in 2017, RMD Open 3 (2) (2017) e000471.

[41] S. Zhong, Q. Ouyang, D. Zhu, et al., Hsa_circ_0088036 promotes the proliferation and migration of fibroblast-like synoviocytes by sponging miR-140-3p and upregulating SIRT 1 expression in rheumatoid arthritis, Mol. Immunol. 125 (2020) 131–139.
[42] J. Salzman, R.E. Chen, M.N. Olsen, et al., Cell-type specific features of circular RNA expression, PLoS Genet. 9 (9) (2013) e1003777.
[43] Y. Jiang, S. Zhong, S. He, et al., Biomarkers (mRNAs and non-coding RNAs) for the diagnosis and prognosis of rheumatoid arthritis, Front. Immunol. 14 (2023) 1087925.
[44] W.Y. Zhou, Z.R. Cai, J. Liu, et al., Circular RNA: metabolism, functions and interactions with proteins, Mol. Cancer 19 (1) (2020) 172.
[45] Y. Xu, F. Chen, Current status of functional studies on circular RNAs in rheumatoid arthritis and their potential role as diagnostic biomarkers, J. Inflamm. Res. 14 (2021) 1185–1193.
[46] Y.H. Pan, W.P. Wu, X.D. Xiong, Circular RNAs: promising biomarkers for age-related diseases, Aging Dis 11 (6) (2020) 1585–1593.
[47] T.B. Hansen, T.I. Jensen, B.H. Clausen, et al., Natural RNA circles function as efficient microRNA sponges, Nature 495 (7441) (2013) 384–388.
[48] X. Geng, C. Zhao, Z. Zhang, et al., Circ_0088036 facilitates the proliferation and inflammation and inhibits the apoptosis of fibroblast-like synoviocytes through targeting miR-326/FZD4 axis in rheumatoid arthritis, Autoimmunity 55 (3) (2022) 157–167.
[49] J.T. Wen, J. Liu, L. Wan, et al., Triptolide inhibits cell growth and inflammatory response of fibroblast-like synoviocytes by modulating hsa-circ-0003353/microRNA-31-5p/CDK1 axis in rheumatoid arthritis, Int. Immunopharm. 106 (2022) 108616.
[50] J. Li, D. Liu, K. Wu, et al., Circ_0003972 promotes the proliferation and inflammation of fibroblast-like synovial cells in rheumatoid arthritis through regulation of the miR-654-5p/FZD4 Axis, Immunol. Invest. 51 (5) (2022) 1437–1451.
[51] H. Li, X. Lin, C. Li, et al., MiR-1286 inhibits lung cancer growth through aerobic glycolysis by targeting PKM2, Arch. Med. Sci. 19 (1) (2023) 151–159.
[52] H. Li, L. Chai, Z. Ding, et al., CircCOL1A2 sponges MiR-1286 to promote cell invasion and migration of gastric cancer by elevating expression of USP10 to downregulate RFC2 ubiquitination level, J. Microbiol. Biotechnol. 32 (7) (2022) 938–948.
[53] M. Muzio, N. Polentarutti, D. Bosisio, et al., Toll-like receptor family and signalling pathway, Biochem. Soc. Trans. 28 (5) (2000) 563–566.
[54] F.G. Bauernfeind, G. Horvath, A. Stutz, et al., Cutting edge: NF-kappaB activating pattern recognition and cytokine receptors license NLRP3 inflammasome activation by regulating NLRP3 expression, J. Immunol. 183 (2) (2009) 787–791.
[55] L. Franchi, T. Eigenbrod, G. Núñez, Cutting edge: TNF-alpha mediates sensitization to ATP and silica via the NLRP3 inflammasome in the absence of microbial stimulation, J. Immunol. 183 (2) (2009) 792–796.
[56] M.S.J. Mangan, E.J. Olhava, W.R. Roush, et al., Targeting the NLRP3 inflammasome in inflammatory diseases, Nat. Rev. Drug Discov. 17 (9) (2018) 688.
[57] L. Zhang, J. Yu, C. Wang, et al., The effects of total glucosides of paeony (TGP) and paeoniflorin (Pae) on inflammatory-immune responses in rheumatoid arthritis (RA), Funct. Plant Biol. 46 (2) (2019) 107–117.
[58] W. Zhai, Z. Ma, W. Wang, et al., Paeoniflorin inhibits Rho kinase activation in joint synovial tissues of rats with collagen-induced rheumatoid arthritis, Biomed. Pharmacother. 106 (2018) 255–259.